# A Vibrational Spectroscopic Study of Molecular Restructuring at Surfaces of Unidirectionally Rubbed Polyimide Thin Films

**Geoffrey D. Hietpas,[†,‡] James M. Sands,[§,||] and David L. Allara*[,†,§]**

*Departments of Chemistry and Materials Science and Engineering, The Pennsylvania State University, University Park, Pennsylvania 16802*

*Received: August 13, 1998*

Rubbing-induced surface reconstruction of the polyimide poly(biphenyl dianhydride-*p*-phenylenediamine) (BPDA-PDA), in the form of 5−300 nm thin films supported on silicon substrates, has been studied using high-precision polarized infrared vibrational spectroscopy in conjunction with spectral simulations. Under unidirectional rubbing, a reversible, selective reorientation of domains of initially well-ordered chains is observed, with the amount of reoriented material equivalent to an ∼1−3 nm thick surface layer, independent of the total film thickness. Accompanying this process are extensive perturbations of the imide ring structures, which include bond distortions of the [O═C−N−C═O] units and out-of-plane rotation of the rings around the chain axis, effectively causing a molecular-scale roughening along the aligned chain axes while maintaining the periodic repeat unit spacing. These effects are proposed to arise from dynamic chain−chain steric interactions that occur as chains align under the applied buffing force. An analogous bulk behavior is shown for the molecular response of unsupported BPDA-PDA films to uniaxial tensile strain. These data provide a new description of the buffed BPDA-PDA polymer surface and thus provide an improved basis for understanding the mechanism of liquid crystal alignment on these surfaces.

## 1. Introduction

Polyimide (PI) materials have had an important role in the manufacture of flat panel liquid crystal displays (LCD's).[1] A key function of the polymer has been its ability to respond to unidirectional buffing so that its surface becomes able to induce alignment of LC molecular overlayers. Since the degree of this alignment is critical to the operation of the final device,[1,2] it is extremely important to understand the underlying alignment mechanism both in terms of the LC−polymer interfacial interactions that induce alignment and the dynamic processes that create the favorable PI surface upon unidirectional rubbing. In this report, we focus on the second aspect.

Past work has shown that the polymer chain axes tend to reorient along the rubbing direction.[3] More recent grazing incidence X-ray diffraction (GIXRD)[4] and near-edge X-ray absorption fine structure spectroscopy (NEXAFS)[5] studies of poly(biphenyl dianhydride-*p*-phenylenediamine) (BPDA-PDA), a rigid, well-ordered polyimide, have shown that the chain realignment occurs in the top ∼5−10 nm surface layer of the polymer, thus establishing the chain reorientation as a surface effect. However, chain reorientation alone has not been sufficient to explain the molecular-level mechanism of the LC alignment.[6] With this in mind, new efforts have focused on other types of molecular changes. Evidence has accumulated recently that buffing of a variety of different types of PI materials, ranging from amorphous to well-ordered, also causes localized perturbations and out-of-plane reorientations of the constituent rings near the surface. In a preliminary report, we showed from polarized infrared difference spectroscopy (PIRDS) data that buffing of rigid, well-ordered BPDA-PDA films causes localized perturbations of the imide rings, including bond distortions and out-of-plane rotations around the main chain polymer axis.[7] Stöhr and co-workers have concluded from NEXAFS data that the buffing of an amorphous PI film induces a small degree of out-of-plane alignment of the phenyl rings and imide −C═O groups.[8] Weiss and co-workers[9] report NEXAFS data on poly(pyromellitimidooxydianiline) (PMDA-ODA), an ordered but less rigid polyimide than BPDA-PDA, that is interpreted as showing a small degree of out-of-plane inclination of the rings upon buffing. These observations highlight the surface tilts and localized structuring of molecular groups as an additional way to develop the basis of LC alignment.[7−9] In particular, the PIRDS results, which specifically suggest molecular-scale localization of ring perturbations, strike a parallel with recent studies of mixed self-assembled monolayers where the localized topographical surface variations of protruding, varying length alkyl chain segments have been shown to change LC alignment, relative to molecularly smooth surfaces.[10] Given the nuances of surface structures that potentially could affect LC alignment, it is clear that systematic work on the quantitative details of the buffing-induced surface restructuring of different types of PI surfaces would be extremely helpful in developing a broadly predictive buffing-induced alignment theory.

Among the most interesting types of PI materials to study with respect to buffing responses are rigid, well-ordered polymers, exemplified by BPDA-PDA, whose chemical structure is given at the top of Figure 1. The ability of such ordered materials to respond to buffing, a low-stress process, is an intriguing and important issue. Given a bulk glass transition temperature several hundred degrees above ambient and given the high thermal-oxidative stability of the polymer,[11] chain axis realignment[4,5,7] at room temperature should not involve simple segmental motion. Since the realignment is clearly restricted to

[†] Department of Chemistry.
[‡] Present address: DuPont Co., Kinston, NC 28502-0800.
[§] Department of Materials Science and Engineering.
[||] Present address: U.S. Army Research Laboratory, Aberdeen Proving Grounds, MD 21005.

10.1021/jp983363i CCC: $15.00 
Published on Web 12/01/1998

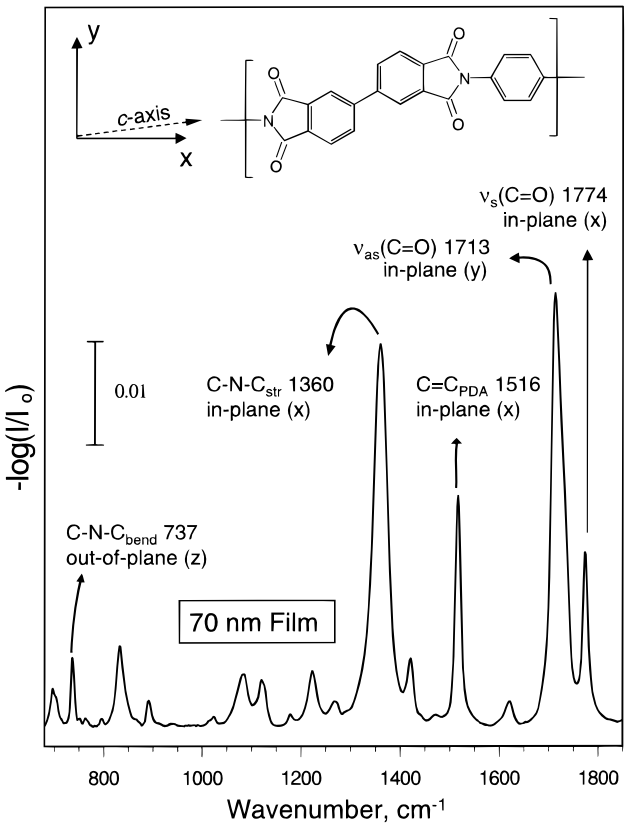


**Figure 1.** Experimental transmission spectrum of a 70.0 ± 0.6 nm imidized BPDA-PDA film supported on a silicon wafer. The diagnostic infrared active modes along with their transition dipole directions are given relative to the molecular frame. The chemical structure of the BPDA-PDA repeat unit and the molecular coordinate directions are given at the top of the figure. The *x,y,z* laboratory frame is indicated in the upper left (*z* is perpendicular to the page). The main chain (*c*) polymer axis is located in the *x,y* plane and is rotated 7.5° from the *x* axis.

the near-surface regions,[4,5] it is important to determine what factors might influence the actual amount of responding chains. Of particular interest are the total film thickness and the initial degree of ordering of the unbuffed film and how these variables will influence the exact character of the changes at the molecular level. Further, it is of interest to determine if there are similar chain and ring reorientations induced during analogous mechanical stresses such as uniaxial drawing. In the present study, we expand on our preliminary report[7] and provide critical molecular-level details of the surface orientational changes that arise during the unidirectional rubbing of an extensive series of BPDA-PDA films of widely varying thickness. The use of the PIRDS characterization technique, which can characterize the amount, chemical state, and orientation of molecular groups, provides an extremely useful complement to the previous GIXRD[4] and NEXAFS[5] analyses of BPDA-PDA. In general, vibrational spectroscopy has been frequently applied to polymer films, including polyimides,[12] because of its high molecular sensitivity. Prior to our preliminary report,[7] few applications to rubbed films had been reported[3] and little quantitative information of the initial and final molecular-level structures was available, especially for the higher rigidity materials. In the present study, thin BPDA-PDA films supported on silicon (native oxide covered) were prepared at selected thicknesses from 5 to 300 nm. The films were prepared and buffed in the same exact manner as for the reported GIXRD study.[4] The details of the infrared spectroscopic characterization of the initial, prebuffed structures have been reported earlier.[13] Building on these results, the present study confirms the earlier picture of a reversible[7] polymer chain axis alignment[4,5,7] and gives values of the total amount of chains involved. Further, the results show in detail the distinct structural perturbations of the BPDA-PDA imide rings that can arise, including out-of-plane ring rotation. Finally, our data show that the amount of material undergoing reconstruction increases with the structural uniformity in the initial, unrubbed sample. The results are explained on the basis of a general mechanism in which domains of ordered chains in the near surface region realign under the applied stress while neighboring chains experience unfavorable steric interactions leading to imide ring restructuring and molecular-scale roughening of the chain stacking plane surfaces. These findings establish a more complete picture of the types of molecular changes that can occur in a buffed surface than previously available and provide an improved basis for developing molecular-level mechanisms of molecular overlayer alignment phenomena.

## 2. Experimental Section

**2.1. Thin Film Preparation and Unidirectional Rubbing.** Details of the film preparation and thickness measurements (from single-wavelength ellipsometry and X-ray reflectivity) have been previously described.[13] The wafers were unidirectionally buffed at room temperature with a velour cloth (74% cotton, 26% polyester) under a constant applied mass of 2 gm/cm$^2$ for a total distance of 300 cm at 0.5 cm/s, following the conditions reported in a recent GIXRD study.[4]

**2.2. Infrared Spectroscopy.** Transmission infrared (IR) spectra were obtained as previously described.[13] Spectra were taken at the selected angle of incidence and combined in various ways depending upon the type of analysis required. The elementary spectral quantities for normal incidence experiments are $I(\|)_U$, $I(\perp)_U$, $I(\|)_B$, $I(\perp)_B$, $I(\|)_{B/U}$, and $I(\perp)_{B/U}$, where $I$ is the spectral intensity at each frequency, B and U refer to buffed and unbuffed samples, and $\|$ and $\perp$ refer to the incident electric field arranged parallel and perpendicular to the selected buffing direction on the sample surface, respectively. To change the alignment of the electric field relative to a selected direction on the sample plane, the sample was rotated relative to a fixed beam polarization direction. The $I$ values were determined as absorbances defined as $I = -\log(T/T_o)$, where $T$ and $T_0$ are the transmitted emission power spectra through the sample and the reference, respectively. For the cases of the $I_U$ and $I_B$ spectra, $T_0$ was obtained using the freshly cleaned, bare native oxide-covered wafer, while for the $I_{B/U}$ cases, $T_0$ was the power spectrum of the unbuffed film sample. For all spectra on a given BPDA-PDA sample, the same exact spot on the surface was analyzed throughout the sample history, starting from the bare wafer prior to casting of the polyamic acid precursor. Failure to follow this protocol inevitably resulted in the appearance of irreproducible spectral artifacts that arise from incomplete corrections for intrinsic Si impurities, optical misalignment, and interference fringing effects.[13] The PIRDS spectral quantity of interest is the difference between the overall buffing responses in the $\|$ and $\perp$ directions, $\Delta \equiv [I(\|)_B - I(\|)_U] - [I(\perp)_B - I(\perp)_U]$. Analysis of the of the separate responses in directions parallel and perpendicular to the rubbing direction was done using the quantities $\Delta\| \equiv I(\|)_B - I(\|)_U$ and $\Delta\perp \equiv I(\perp)_B - I(\perp)_U$. Although all the BPDA-PDA thin films analyzed were essentially fully optically isotropic in the film plane,[13] the magnitudes of the observed PIRDS spectra for these samples were sufficiently small that even otherwise minor differences of the unbuffed spectra for different polarization directions had to be specifically

calibrated by accurate determination of the quantities $I(\|)_{(U)}$ and $I(\perp)_{(U)}$ prior to analysis of the effects of unidirectional rubbing.[14]

**2.3. Quantitative Spectral Analysis.** A general electromagnetic treatment of the transmission and reflection of light through a multilayered system, in which one or more of the layers is both absorbing and anisotropic, has been developed.[15] For the thin polymer films supported on silicon presented here, each layer in the multilayer sample is described by a directionally dependent, complex optical function tensor spectrum. These input data are used to compute a simulated spectrum by application of a $4 \times 4$ transfer matrix that relates the electric field amplitudes within each layer. The computations utilized a previously published[16] adaptation of the Yeh formalism[15] that was developed for spectroscopic applications. Additional details relevant to the specific case of the highly anisotropic BPDA-PDA films are given in a companion paper.[13]

To simulate accurately a specific experimental difference spectrum, three steps were followed. First, a simulated transmission spectrum, $I_U = I(\|)_U = I(\perp)_U = (T/T_0)$ was calculated for an initial (unrubbed) supported BPDA-PDA film of thickness $d$ using the six-medium system [air/film(3−2000 nm)/$SiO_2$(2 nm)/Si($1 \times 10^6$ nm)/$SiO_2$(2 nm)/air]. Since the film is unrubbed, it can be accurately treated as totally isotropic in the surface plane (uniaxial symmetry).[13,17] The reference ($T_0$) was defined as the corresponding five-medium system [air/$SiO_2$/Si/$SiO_2$/air].[18] Second, $I(\|)_B = [T(\|)/T_0]$ and $I(\perp)_B = [T(\perp)/T_0]$ spectra were calculated for the electric fields aligned parallel and perpendicular, respectively, to the $c$ axis of a polyimide chain using the seven-medium system [air/film($x$)/film($d-x$)/$SiO_2$/Si/$SiO_2$/air], which contains an oriented BPDA-PDA layer of thickness $x$ located on top of the original, uniaxial BPDA-PDA film, now of reduced thickness ($d - x$). In all cases, the buffing direction was defined as the $c$-axis direction of the PI chains. Third, the spectral quantities $\Delta\| = [I(\|)_B - I_U]$, $\Delta\perp = [I(\perp)_B - I_U]$, and $\Delta = \Delta\| - \Delta\perp$ were determined and compared with the corresponding experimentally determined spectra. Following these steps, if the fits between the experimental and the simulated spectra from step three were not acceptably close, then the simulation process was repeated with changes in $x$ and/or uniform out-of-plane twisting of the imide rings as variable parameters in the fitting iterations.

The optical function tensor spectra for the simulations were obtained from 3 $\mu$m free-standing film data reported earlier.[13] The C−N−$C_{bend}$, C═$C_{PDA}$, and $\nu_s$(C═O) matrix elements represent only in-plane responses and the scalar values were used directly as reported. The $\nu_{as}$(C═O) mode may be described by three components: planar conjugated, $\upsilon^o$, pertrubed rings that remain in-plane, $\nu^*_{in}$, and perturbed rings twisted out-of-plane, $\nu^*_{out}$. For the in-plane normal incidence transmission spectra presented here, $\nu^*_{out}$ was ignored. The general simulation procedure consisted of adjusting the contributing proportions of these three modes in the overall $\nu_{as}$(C═O) optical function in order to match the observed overall $\nu_{as}$(C═O) spectral line shape of the specific sample of interest before buffing. The identical optical function was applied to simulations of the buffed sample with changes made only for sample rotation in the $x,y$ plane.

## 3. Results

**3.1. Initial Film Structure.** The initial film structure of the samples used in this study is described in detail elsewhere,[13] and only those aspects relevant to an analysis of the unidirectional rubbing processes are reviewed here. The molecular structure of the BPDA-PDA repeat unit, along with a representative IR spectrum for the case of a $70.0 \pm 0.6$ nm film, are shown in Figure 1. Also shown are the typical frequencies and the transition dipole moment directions for selected vibrational modes that are characteristic of the imide and the *p*-dianiline (PDA) rings. These modes are centered near 1774 [symmetric imide stretch, $\nu_s$(C═O) or symmetric imide I], 1714 [antisymmetric imide stretch, $\nu_{as}$(C═O) or antisymmetric imide I], 1516 (C═C tangential stretch of the PDA ring, C═$C_{PDA}$), 1360 [C−N−C axial stretch, C−N−$C_{str}$, or imide II], and 737 $cm^{-1}$ (C−N−C out-of-plane bending, C−N−$C_{bend}$, or imide IV). The transition dipole directions that are parallel to the respective ring planes are labeled as either parallel to the $x$ or $y$ axes, where $x$ is defined in the figure as the N−$C_6H_4$−N bond axis of the PDA group. Note that the actual chain axis is tilted ∼7.5° away from the $x$ axis.

In the companion study, it was concluded[13] that the structure of unbuffed BPDA-PDA films supported on silicon wafers, prepared in the manner used in the present study, fits the generally accepted picture of planar stacks of parallel-aligned, linearly extended chains with periodic chain−chain spacings across the stacking layers. This structure would correspond to the $x,y$ plane in Figure 1 being parallel to the stacking plane. While the chain axes are aligned quite parallel to the substrate surface, the in-plane ($x,y$) alignment is isotropic, which indicates that the stacking planes consist of domains randomly oriented in the surface plane. However, in addition to this generally accepted picture, the IR data show that a significant fraction of the *imide* rings associated with these well-ordered chain structures actually exhibit perturbed structures that involve both out-of-plane (surface plane) rotation and conformational or bond distortions. The existence of these perturbed structures was characterized by the appearance of a new imide I antisymmetric C═O stretch, $\nu^*_{as}$(C═O), near 1728 $cm^{-1}$, which has both in-plane and out-of-plane components, $\nu^*_{in}$ and $\nu^*_{out}$. In consideration of this complexity, the intrinsically unperturbed mode associated with planar imide rings is designated as $\nu^o_s$ or $\nu^o_{in}$ (to signify the pure in-plane character). It was observed that the degree of imide ring perturbations decreases with decreasing thickness. However, the fact that significant residual contributions exist, even in the thinnest films (several nanometers), indicates that the best preparations of these films show strong, localized imide ring packing perturbations, despite the high degree of overall chain axis ordering indicated by GIXRD patterns.[4] The top- and side-view structures shown on Figure 2A represent a schematic of the unbuffed BPDA-PDA thin film structure based on the above conclusions from the earlier study.[13]

**3.2. Unidirectional Rubbing.** *3.2.1. Analysis of* Δ *Spectra: Deviations from Simple Chain Axis Reorientation.* Normal incidence PIRDS spectra [$\Delta = \Delta\| - \Delta\perp$], are shown in Figure 3 (solid lines) for films of seven different thicknesses. The normal incidence spectra are sensitive only to structural changes associated with modes possessing transition dipole moment components in the sample surface plane. For the analysis that follows, it is first useful to examine the ideal results that would be obtained for in-plane ($x,y$, Figure 1) reorientation of a single chain along the buffing direction with each of the molecular units left intact, i.e., with no bonding or conformational distortions. The predicted qualitative responses, based on the transition dipole directions given in Figure 1 and in the previous section, are listed in Table 1. The results in the table would be obtained for the ideal case of well-ordered BPDA-PDA thin films with the chains aligned in a planar stacking configuration and the ring planes parallel to the surface. These predictions roughly hold, as seen in Figure 3, and are entirely consistent with the well-established fact that the BPDA-PDA chains align

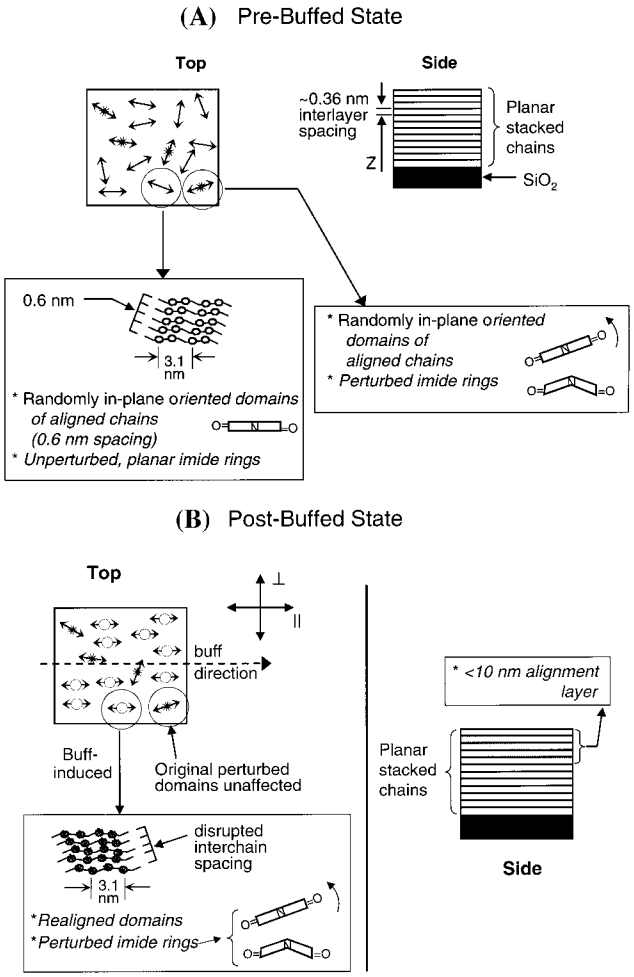


**Figure 2.** Schematic showing the initial film structure in the *x,y* plane (**A**) before and (**B**) after rubbing, as derived from a combination of the present infrared data and published X-ray probe data (for details see text). The cartoons representing the response of the imide rings to the rubbing process show how a planar unperturbed region of arbitrary orientation is rotated in-plane along the rubbing direction and perturbed in the process.

parallel to the buff direction.[4,7] This aspect is illustrated in the schematic in Figure 2B. A closer examination of Figure 3, however, shows evidence for nonideal behavior, for example, the appearance of relatively small C−N−$C_{bend}$ out-of-plane mode features (expanded scale inset) and a complex $\nu_{as}$(C═O) band with multiple components. These types of deviations are the focus of this work and will form the basis of the analyses below.

*3.2.2. Analysis of the Individual* Δ|| *and* Δ⊥ *Spectra.* To analyze separately the directional components of the observed chain restructuring, the quantities $\Delta\| = [I(\|)_B - I(\|)_U]$ and $\Delta\perp = [I(\perp)_B - I(\perp)_U]$ were calculated from the data. The results are shown in Figures 4 and 5.

*3.2.2.1. Overall Intensity Comparisons: Evidence for No Loss of Polymer Upon Buffing.* An important point to note is that the average of the component $I(\|)_B$ and $I(\perp)_B$ spectra for any given thin film is always approximately equal to the $I(\|)_U$ spectra. This result shows that all the initial oscillator intensity is essentially accounted for in the || and ⊥ spectra. This requires that no loss of polyimide material occurs under our buffing conditions. This conclusion is corroborated by the invariance of the ellipsometric and X-ray reflectivity thicknesses with buffing. Given our experimental errors for thicknesses and IR intensities, we estimate that no more than a fraction of a nanometer of surface could be removed (~1 layer of chains).

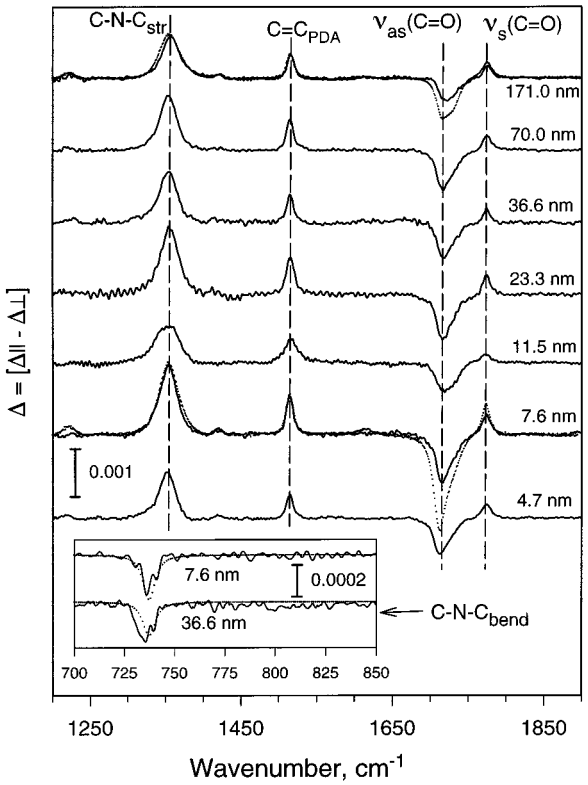


**Figure 3.** Δ spectra for BPDA-PDA films of different thicknesses. The dotted lines (7.6 and 171.0 nm films) represent simulated spectral bands for a layer of chains realigned along the buff direction. The simulations are based on unbuffed film optical function spectra except for corrections to the complex $\nu$(C═O) mode relative intensities. The thicknesses of the reorientation layers, as determined from fits of the C−N−$C_{str}$ and C═$C_{PDA}$ bands, are 2.8 and 1.8 nm for the 7.6 and 171.0 nm films, respectively. For details see text.

**TABLE 1: Predicted Magnitudes of PIRDS, Normal Incidence Spectral Quantities for the Different Diagnostic Modes of a BPDA-PDA Chain that Aligns Parallel to the Buffing Direction**[a]

| mode | ~$\nu$ (cm$^{-1}$) | transition moment direction in molecular frame (see Figure 1) | predicted spectral response for normal incidence | | |
|---|---|---|---|---|---|
| | | | Δ\|\| | Δ⊥ | Δ |
| C−N−$C_{bend}$ | 737 | *z* | 0 | 0 | 0 |
| C−N−$C_{str}$ | 1360 | *x* | + | − | + |
| C═$C_{PDA}$ | 1516 | *x* | + | − | + |
| $\nu_s$(C═O) | 1774 | *x* | + | − | + |
| $\nu_{as}$(C═O) | 1713−1728 | | | | |
| $\nu^o$ | 1713 | *y* | − | + | − |
| $\nu^*$ | 1728 | | | | |
| $\nu^*_{in}$ | | *y* | − | + | − |
| $\nu^*_{out}$ | | *z* | 0 | 0 | 0 |

[a] The predictions assume that the chain reorients as an integral unit and that the molecular groups undergo no local perturbations. The spectral quantities and modes are defined in the text.

*3.2.2.2. Derivative-Like Band Shapes: Evidence for Multiple Structural Responses to Buffing.* For the C−N−$C_{str}$ and C═$C_{PDA}$ modes (~1360 and 1516 cm$^{-1}$, respectively), derivative-like line shapes are observed for both Δ|| and Δ⊥ peaks and the major intensity component of the peaks is positive and negative, respectively, for the two polarization directions. The presence of both signs implies that there are multiple structural responses to buffing and one can presume these to be associated with more than one type of initial structure in the unbuffed film, a point considered further in section 3.2.3. One observes in Figures 4 and 5 that the *dominant* portion of each mode peak

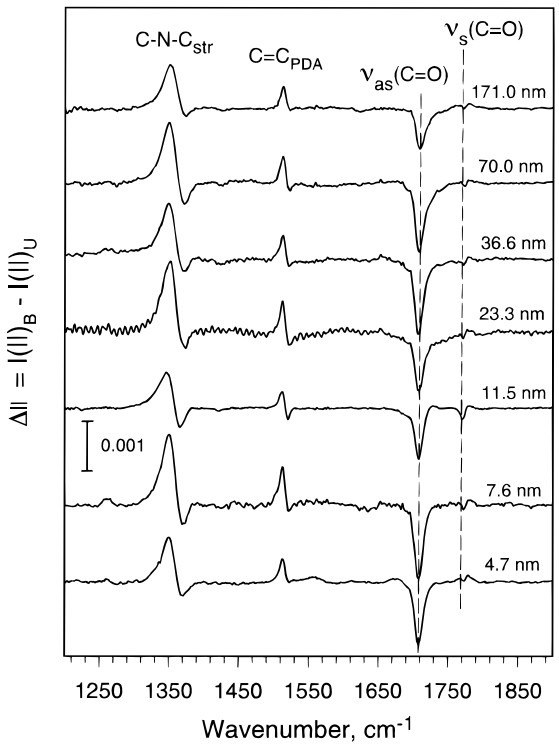


**Figure 4.** $\Delta||$ spectra for BPDA-PDA buffed films of different thicknesses.

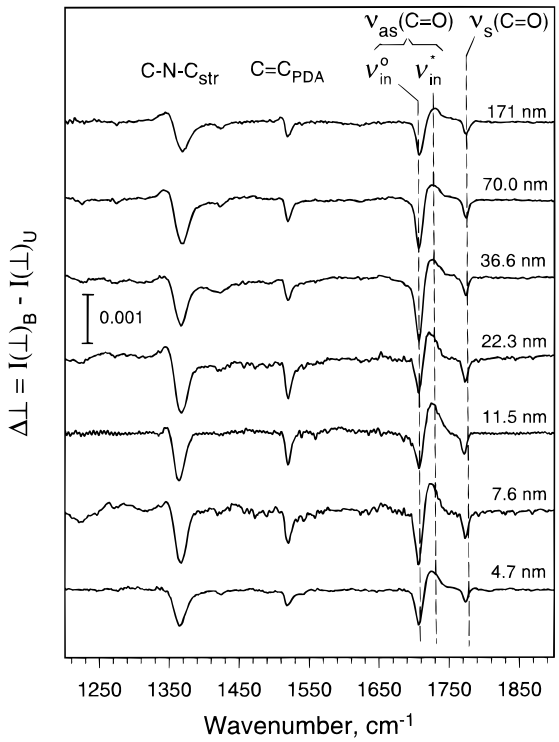


**Figure 5.** $\Delta\perp$ spectra for BPDA-PDA buffed films of different thicknesses.

behaves in an ideal way, according to the qualitative predictions in Table 1. However, a more quantitative analysis shows significant deviations from ideal behavior.

The location of the major peak component of the C−N−C$_{str}$ and C═C$_{PDA}$ modes is different in each directional spectrum, viz., 1350.7 and 1513.0 cm$^{-1}$ for $\Delta||$ but 1366.7 and 1519.4 cm$^{-1}$ for $\Delta\perp$, a shift of ∼16 and ∼8 cm$^{-1}$, respectively. This result suggests that the local environment of those chains that undergo realignment is perturbed to some extent in response to the rubbing process, and the larger shift for the C−N−C$_{str}$ mode suggests that the imide ring is affected to a greater extent than the PDA ring. Note that these shifts for the individual directional spectra, $\Delta||$ and $\Delta\perp$, are larger than in the difference $\Delta$ spectra given in Figure 3. The similar appearance of the $\Delta$ to the initial unbuffed film spectra arises because of the cancellation of the $\Delta||$ and $\Delta\perp$ derivative shapes when the two are subtracted to form $\Delta$.

The strongest support for disruptions of the chain environments is obtained from analysis of the anomalous behavior of the $\nu_{as}$(C═O) and $\nu_s$(C═O) modes (Figures 4 and 5; 1700−1800 cm$^{-1}$ region).

First we consider $\nu_{as}$(C═O), which consists of components $\nu^o_{in}$ and $\nu^*_{as}$, associated respectively with unperturbed imide rings aligned parallel to the surface plane and with an ensemble of perturbed imide rings. The $\nu^*_{as}$ mode consists of in- and out-of-plane components $\nu^*_{in}$ and $\nu^*_{out}$. The components are associated respectively with transition moments oriented along the *x* and *y* directions, designated as $M^y_{as}$ and $M^z_{as}$.[13] Note that $\nu^*_{out}$ is not considered in the analyses below since it is inactive in the normal incidence spectra.

Figure 4 shows that $\Delta||(\nu^o_{in}) < 0$ (∼1700 cm$^{-1}$), as expected from the prediction in Table 1. However, note that while ideal behavior (Table 1) gives $\Delta\perp(\nu^o_{in}) > 0$, *in striking contrast*, experiment shows $\Delta\perp(\nu^o_{in}) < 0$, as seen in Figure 5. Figure 5 also shows a feature near 1730 cm$^{-1}$ within the $\Delta\perp[\nu_{as}$(C═O)] band, which we assign to the $\nu^*_{in}$ mode associated with perturbed imide rings. In contrast to the $\nu^o_{in}$ mode, the $\nu^*_{in}$ mode instead follows the predicted behavior in Table 1. Note also the intriguing behavior that, except for the thinnest film of 4.7 nm, this feature appears to *increase* in intensity with decreasing film thickness.[19]

We interpret this seemingly anomalous behavior in terms of destruction and creation of oscillators via buffing-induced perturbations. First, consider the $\nu^o_{in}$ mode of unperturbed, planar imide rings. Since it is unambiguous that reorientation of a chain aligns its axis (*x* direction) parallel (||) to the buffing direction, then the pure y transition moment $[M_{C=O}(\nu^o_{in}) = M^y_{C=O}(\nu^o_{in})]$ is forced $\perp$ to the buff axis. Thus, the only way to defeat the ideal behavior (Table 1), viz., to avoid $I(\perp)_B > I(\perp)_U$, is for the number of $\nu^o_{in}$ oscillators responding to the IR radiation to *decrease upon buffing*. This could occur by a conversion of unperturbed imide rings (associated with $\nu^o_{in}$) to perturbed rings [associated with ($\nu^*_{in}$, $\nu^*_{out}$)]. The conservation of imide groups involved in the buffing requires

$$n^o_{in}(U) \xrightarrow{buff} n^*_{in}(B) + n^*_{out}(B) + n^o_{in}(B)$$

where *n* equals the total number of each type of oscillator before and after buffing. It is useful to define the conversions in terms of fractions: $f^*_{in} = \nu^*_{in}(B)/\nu^o_{in}(U)$ and $f^*_{out} = \nu^*_{out}(B)/\nu^o_{in}(U)$ with $f^* = f^*_{in} + f^*_{out}$ = the fraction of initial $\nu^o_{in}$ oscillators lost via conversion. Since complete $\perp$ alignment of initially in-plane isotropic $\nu^o_{in}$ oscillators would result in $I(\perp)_B = 2I(\perp)_U$ or $\Delta\perp = +I(\perp)_U$, inclusion of the loss of $\nu^o_{in}$ oscillators gives

$$\Delta\perp(\nu^o_{in}) = f^*2I(\perp)_U - I(\perp)_U = (1 - 2f^*)I(\perp)_U$$

Accordingly, when $f^* > 0.5$, $\Delta\perp(\nu^o_{in}) < 0$. Thus, the experimental observation of a negative $\Delta\perp(\nu^o_{in})$ peak can be rationalized on the basis of greater than 50% loss of $\nu^o_{in}$ oscillators. This process is also consistent with the observations of (1) $\Delta\perp(\nu^*_{in}) > 0$ (Figure 5), since $I(\perp,\nu^*_{in})$ increases on

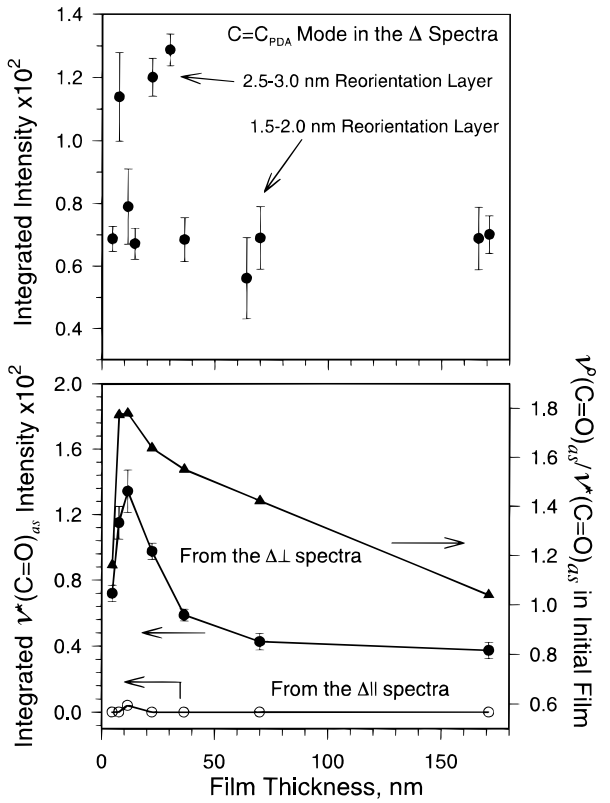


**Figure 6.** (Top) plot of the integrated intensities of the C═C$_{PDA}$ mode in the Δ spectra versus film thickness. (Bottom) (Δ) plot of the relative content of unperturbed, planar imide rings in the thin films as a function of film thickness, shown as the integrated intensity ratio of the $\nu^{o}_{as}$-(C═O) and $\nu^{*}_{as}$(C═O) mode peaks. (●) and (○): plots of the integrated intensities of the $\nu^{*}_{as}$(C═O) component in the Δ⊥ and Δ|| spectra, respectively. As a guide to the eye, a line has been drawn through the individual points in each plot.

buffing; (2) $\Delta\|(\nu^{o}_{in}) < 0$ (Figure 4), since both *loss* of $\nu^{o}_{in}$ oscillators and realignment give this result, and (3) $\Delta\perp(\nu^{*}_{in}) > 0$ features (Figure 5), since both *creation* of $\nu^{*}_{in}$ oscillators and chain realignment give this result. Note that the idealized structures of the buffing layer, given in Figure 2B, show complete conversion of the imide rings for convenience of presentation.

*3.2.2.3. Effects of Film Thickness Variations: Evidence for Domains of Chains Unresponsive to Buffing.* As seen in Figures 3, 4, and 5, the Δ spectra show small variations with film thickness. This effect was examined in detail using the C═C$_{PDA}$ peak, since this mode is minimally affected by typical structural perturbations in well-ordered BPDA-PDA films.[13] Figure 6 (top) shows that the observed integrated Δ(C═C$_{PDA}$) peak intensities for a number of different samples vary with film thickness (data from Figure 5) in a bimodal way for sample thicknesses under 40 nm. Figure 6 also shows values for equivalent buffing response layer thicknesses that were determined from spectral simulations (details given in Section 3.3).

In our previous study,[13] it was shown that as the film thickness of unbuffed films decreases, the degree of local structural perturbations of the imide rings decreases with the rings approaching the ideal planar, stacked structure. We examine this point in some detail in Figure 6 (bottom) where the ratios of the integrated $\nu^{o}_{as}$ to $\nu^{*}_{in}$ peak intensities, $(I^{o}/I^{*})_{U}$, in the initial unrubbed film spectra (spectra not shown for brevity) are plotted as a function of total film thickness. At ∼6.0 nm, $(I^{o}/I^{*})_{U}$ reaches a maximum and then decreases with increasing film thickness. Increases in $(I^{o}/I^{*})_{U}$ can be presumed to follow increases in the fraction of planar, unperturbed imide rings (associated with $\nu^{o}_{as}$) in the film; thus, the maximum film organization is reached at ∼6 nm. The accompanying plot of the integrated Δ⊥ intensity of the $\nu^{*}_{in}$ peak for the buffed film also shows a maximum at a similar film thickness of ∼10 nm. Thus, at this thickness, there appears to be a maximum in the extent of rubbing-induced imide ring perturbations.

The implication of the similarity in the above two plots is straightforward; *the more well-structured and planar the initial film, the greater the extent of imide ring perturbation imparted in the buffing-induced reorientation layer*.

Figure 6 also shows that after buffing, $\Delta\|(\nu^{*}_{in}) \approx 0$; thus, $I(\|,\nu^{*}_{in})_{B} \approx I(\|,\nu^{*}_{in})_{U}$. This result implies a rather significant conclusion. Utilizing the analysis in Table 2, consider two possible limiting cases of imide ring changes upon chain realignment parallel to the buffing direction. First, for conversion of initially unperturbed to perturbed imide rings ($\nu^{o}_{as} \rightarrow \nu^{*}_{in}$, $\nu^{*}_{out}$), with only the $\nu^{*}_{in}$ modes active in the normal incidence spectra, one expects $\Delta\|(\nu^{*}_{in}) = 0$, as is observed. However, consider the case of chain realignment involving *initially perturbed* imide groups, with spectral intensity $I(\|,\nu^{*}_{in})_{U}$, where no change in the character of $\nu^{*}_{in}$ modes occurs during realignment. In this case, since $I(\|,\nu^{*}_{in})_{B} < I(\|,\nu^{*}_{in})_{U}$, $\Delta\|(\nu^{*}_{in}) < 0$, in *contradiction* to the observed positive peak (Figure 4). The general conclusion from this analysis is that any chains *initially* present in a disordered configuration *do not respond* to the rubbing process.

The basis of this Δ|| intensity analysis and the experimental results are summarized in Table 2 along with consideration of additional cases of imide ring perturbation possibilities and resultant effects on Δ⊥ intensities for different initial chain orientations. From this table, it is seen that the only possible way to obtain the experimentally observed Δ|| and Δ⊥ intensities is if the initially perturbed imide rings do not change in response to unidirectional rubbing, while the realignment of initially unperturbed, planar imide rings produces a significant conversion to perturbed rings. Since the in-plane reorientation of imide rings can arise only by chain realignment, the lack of reorientation of initially perturbed rings on buffing means that the chains associated with these imide rings do not respond to buffing. Further, since the in-plane motions of the polymer chains must be correlated, especially in domains with well-aligned chains, one can conclude that the *initially perturbed imide rings must exist predominantly in specific domains distinct from other domains of chains bearing unperturbed, planar imide rings*. This feature of the buffing mechanism is also seen in the schematic in Figure 2.

*3.2.2.4. Off-Normal Incidence Spectra: Evidence for Buffing-Induced, out-of-Plane Ring Twisting.* The above results strongly suggest that buffing induces local disorder of initially unperturbed, planar imide rings. Since this effect is expected to include ring twisting out of the surface plane,[13] a series of *p*-polarized transmission spectra were taken at a 60° incidence angle in order to check the out-of-plane spectral changes induced by buffing. To explore the effects of the extent of initial imide ring perturbation, two films of similar thickness, nominally in the 10 nm range, were prepared to have different contents of perturbed imide rings. A 11.5 nm film was made in the standard way, while a series of other films were made by arbitrarily varying cure rates well outside of the standard value. A 9.0 nm film was selected as the companion film. Using our earlier analysis,[13] the IR spectra (not shown) indicated that the 9.0 nm film contains a considerably larger fraction of perturbed imide rings relative to the 11.5 one. Figure 7 shows that the Δ⊥ spectra

**TABLE 2: Experimental and Predicted Behavior of the Imide Ring C═O Antisymmetric Stretching Mode Peak Intensity in the Polarized Buffing Effect Spectra for Different Initial BPDA-PDA Chain Configurations**

| buffing response model | initial chain axis direction relative to buff direction | peak intensity in normal incidence polarized buffing effect spectra for $\nu^{o}_{as}$(C═O) and $\nu^{*}_{as}$(C═O) modes (~1709 and 1726 cm$^{-1}$, respectively) | | | |
|---|---|---|---|---|---|
| | | $\Delta\parallel = [I(\parallel)_B - I(\parallel)_U]$ | | $\Delta\perp = [I(\perp)_P - I(\perp)_U]$ | |
| | | $\nu^{o}_{as}$(C═O) | $\nu^{*}_{as}$(C═O) | $\nu^{o}_{as}$(C═O) | $\nu^{*}_{as}$(C═O) |
| $\nu^{o} \rightarrow \nu^{o}$ | ∥ | 0 | 0 | 0 | 0 |
| | 45° | − | 0 | + | 0 |
| | ⊥ | − | 0 | + | 0 |
| $\nu^{*} \rightarrow \nu^{*}$ | ∥ | 0 | 0 | 0 | 0 |
| | 45° | 0 | − | 0 | + |
| | ⊥ | 0 | − | 0 | + |
| $\nu^{*} \rightarrow \nu^{o}$ | ∥ | 0 | 0 | + | − |
| | 45° | 0 | − | + | − |
| | ⊥ | 0 | − | + | 0 |
| $\nu^{o} \rightarrow \nu^{*}$ | ∥ | 0 | 0 | − | + |
| | 45° | − | 0 | − | + |
| | ⊥ | − | 0 | 0 | + |
| experimental spectra (Figures 4 and 5) | | − | 0 | − | + |

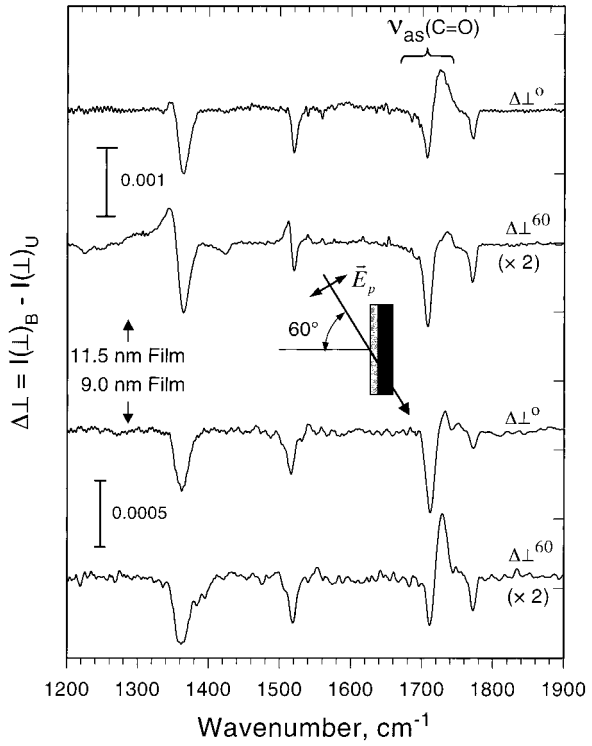


**Figure 7.** $\Delta\perp$ spectra for 11.5 and 9.0 nm thin films. The spectra were obtained at a 60° angle of incidence using *p*-polarized light. The peak location of the imide I antisymmetric stretch associated with perturbed imide rings $\nu^{*}_{as}$(C═O) is indicated in the top spectrum by an arrow. The initial, unrubbed 9.0 nm film was prepared in a manner to provide a much higher extent of perturbed imide rings than the 11.5 nm film, as shown by the larger $\nu^{*}_{as}$(C═O) peak for the former: for details see text. The inset shows the experimental arrangement with the direction of electric field polarization of the *p*-polarized light.

intensity ratio of the composite $\nu^{*}_{as}$ peaks (at ~1728 cm$^{-1}$) at 60° and 0° (normal) incidence is nearly an order of magnitude larger (note scale differences in the figure) for the initially more perturbed 9.0 nm film. Since the off-normal spectra carry out-of-plane (*z*) information, the simple conclusion is that the *contribution of out-of-plane twisting to the total buffing-induced perturbations of the imide rings is significantly larger when the intrinsic perturbation of the unbuffed film is greater*.

*3.2.3. Unidirectionally Drawn, Unsupported Films: A Close Analogy to Buffing.* In the difference spectra presented above, the presence of multiple components was typically observed in most of the diagnostic bands, as manifested in derivative-like features at the band edges. These features arise as a result of correlated chain reorientations in ordered domains, an unexpected process in view of a sample temperature nearly several hundred degrees below the bulk $T_g$. To gain more insight into this behavior, an analogous system of a uniaxially stretched free-standing BPDA-PDA film was studied. Films were prepared at ~3 $\mu$m thicknesses. The initial spectra were recorded, the films then were uniaxially strained at room temperature to a point just below tensile failure, and spectra were again recorded. Finally, the tensile force was removed, and a final $\Delta$ spectra was taken after 24 h. The results show that the tensile and buffing behavior of the films is highly analogous.

The results for a 3.5 $\mu$m film are shown in Figure 8. Note that the overall line shapes are quite similar to those observed in the $\Delta$ spectra for the buffed thin films. For modes with *x* direction transition moments, C−N−$C_{str}$, C═$C_{PDA}$, and $\nu_s$(C═O), $\Delta$ is greater than 0, while for the *y* direction mode, $\nu_{in}$(C═O), $\Delta$ is less than 0. These results follow the ideal behavior in Table 1, with the substitution of draw direction for buff direction. Also note that the intensity of the peaks are all ~0.03 of the intensities of the corresponding ones in the spectrum of the unstrained film. This indicates a significant fraction of chains realign on drawing. One should note that in the drawing case, chains align throughout the bulk with the total amount proportional to the volume of the sample. In contrast, for the surface buffing, essentially only a constant amount of chains align, regardless of the sample thickness (see previous and subsequent sections).

It is interesting that $\Delta$ is less than 0 for the C−N−$C_{bend}$ mode (~738 cm$^{-1}$), whereas the ideal behavior for a perfect in-plane strain would show no response for this *z* direction mode (Table 1). This result indicates that uniaxial alignment of the chains causes some twisting of the imide ring planes out of the film surface plane. This is analogous to the buffing behavior of this mode for which a weak $\Delta$(C−N−$C_{bend}$) < 0 peak is observed (Figure 3).

Figure 8 also shows the $\Delta$ spectrum for the same sample left for 24 h at ambient temperature after the tensile force was removed. One can clearly see that additional chain segmental motion has occurred and that the degree of orientation along the drawing direction has increased. The latter effect shows that, in the absence of an external drawing force, the aligned chains already present can serve as an ordering template for further

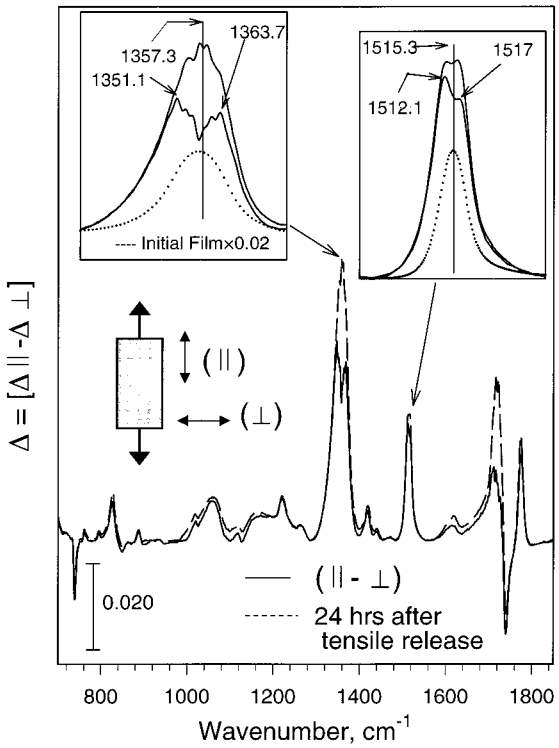


**Figure 8.** Δ spectra for a free-standing, ~3.5 $\mu$m thick BPDA-PDA film after uniaxial drawing just below the tensile failure point at room temperature. The dashed line is the same spectrum for the sample 24 h after removal of the tensile force. The inset shows that the C−N−$C_{str}$ and C═$C_{PDA}$ mode peaks (see text) are split into multiple components. In addition, the dotted lines in the insets show the unstretched film spectra.

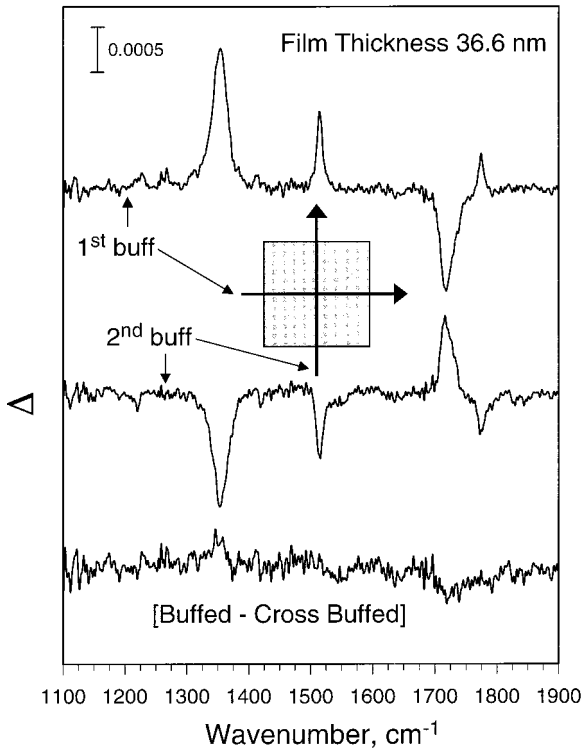


**Figure 9.** Δ spectra for a 36.6 ± 0.5 nm BPDA-PDA film that has been buffed in one direction and then buffed again in a perpendicular direction (cross-buffed). The bottom spectrum is the sum of the above two spectra, and the null value indicates that a constant amount of material is involved in the rubbing and cross-rubbing processes. In calculating the $I(\perp)$ and $I(\parallel)$ spectra of the cross-rubbed sample from the individual sample and reference spectra, the || direction on the wafer was kept to the initially selected one; for details see text.

chain orientation. This phenomenon has been previously observed for micrometer thickness polyimide films using Young's modulus measurements on thermally drawn films and films drawn at the unimidized polyamic acid stage.[22]

The presence of multiple components in the stretched film for each of the diagnostic modes can be clearly observed from Figure 8. The inset shows an expanded region for the C−N−$C_{str}$ and C═$C_{PDA}$ modes that occur at 1357 and 1515 $cm^{-1}$, respectively, in the initial transmission spectrum. For the C−N−$C_{str}$ mode, at least six components can be observed in the Δ spectra for the drawn sample. This peak splitting is interpreted as multiple configurational states of the imide rings. The differences in these states are attributed to changes in the bonding and electronic structure of the imide [O═C−N−C═O] group, similar to the changes typically observed and monitored in protein secondary structure determinations.[21] For the C═$C_{PDA}$ mode, a doublet splitting into peaks at 1512 and 1517 ± 2 $cm^{-1}$ also is observed with variations arising for different samples at different drawing forces. These features are similar to those that were observed separately in the Δ|| and the Δ⊥ spectra of buffed films (Section 3.2.2, Figures 4 and 5). For both of these modes in the drawn samples, Figure 8 (inset) shows that the strain-induced splittings gradually decrease upon release of the tensile force and the spectra gradually revert to those initially observed prior to drawing. To our knowledge, these are the first direct measurements of mechanically induced segmental motion at room temperature for the BPDA-PDA polyimide. We conclude from the overall parallel behavior of drawing and buffing that these complex chain response and relaxation effects also occur in buffing. However, because of the small amount of material involved in buffing, the effects are too weak to be readily observed.

*3.2.4. Cross-Rubbed Films: Evidence for Chain Realignment as a Reversible Process.* To test the reversibility of chain reorientation in the buffing process, experiments were conducted in which sequential buffing operations were performed for alternating buffing directions. A two-step process is sufficient to show the observed reversibility. Figure 9 shows the Δ spectra for a selected example of a 36.6 ± 0.4 nm film that has been rubbed (||) and then cross-rubbed in a perpendicular direction (⊥). Simple inspection of the peak areas shows that a nearly identical amount of film material is modified in each case. For further analysis of the result, consider the C−N−$C_{str}$, C═$C_{PDA}$, and $\nu_s$(C═O) modes, which all have the *x* direction transition moments (Figure 1). From Table 1, we expect $\Delta > 0$. The $\Delta < 0$ peaks observed upon cross-buffing, seen in Figure 9, demonstrate that the *chains realign again on the cross-buff*. This striking reversibility of the chain orientation suggests that the *alignment layer is quite mobile*, with no apparent tendency to rigidify along the rubbing direction, and *consists of a near constant quantity of material*. This behavior is quite general for a variety of samples of different thicknesses (data not shown) and for multiple cross-buffs.

**3.3. Spectral Modeling of the Realignment Layer: Estimation of the Amount of Polymer which Realigns on Buffing.** Spectral modeling was performed in order to quantitate the amount of material that responds to the buffing process. The normal incidence Δ spectra of the 7.6 and 171.0 nm films, shown in Figure 3, were simulated using the methods described in section 2.3. First, simulations were made of the initial unrubbed film spectra using an optical function derived directly from the previously determined in-plane function $\hat{n}(\nu)_{in}$.[13] Since each initial unrubbed film can exhibit different relative intensities

of the $\nu^{o}_{as}$ and $\nu^{*}_{as}$ modes, representative of the extent of intrinsic imide ring perturbation,[13] the in-plane optical tensor ratio, $\hat{n}(\nu)_{in}$ $(\nu^{o}_{in})/\hat{n}(\nu)_{in}(\nu^{*}_{in})$, for each sample was adjusted until the simulations matched the observed individual line shapes. Following this, the entire $\hat{n}(\nu)_{in}$ function (including the $\nu^{o}_{as}$ and $\nu^{*}_{as}$ modes) was used for simulation using the experimental film thicknesses. This procedure, as expected, gave excellent matches to the observed spectra of the unbuffed samples.

Next, to simulate the buffed film spectra, it was assumed that all the chains in a layer of thickness *x* were aligned, with the remainder isotropic in the *x,y* plane. Using the above optical functions, the || and ⊥ buffed film spectra were calculated for variable values of *x* until satisfactory fits of the Δ spectra were obtained for the intensities of the C−N−$C_{str}$ and C═$C_{PDA}$ modes. The best-fit equivalent realignment layer thicknesses for the 7.6 and 171.0 nm films are ∼2.8 and 1.8 nm, respectively (Figure 3, dotted lines). These values are well within the range suggested by previous X-ray measurements.[4,5]

One can note the poor match of the $\nu_{as}$(C═O) and the $\nu_{s}$(C═O) mode peaks. Since the optical function $\hat{n}(\nu)_{in}$ was never varied during the fitting procedure, except to account for sample orientation, the poor fits of these features support our previous conclusions of induced imide ring structural perturbations during rubbing.

Given that the C−N−$C_{str}$, C═$C_{PDA}$, and $\nu_{s}$(C═O) modes all have *x* direction transition moments, ideally, the good fits of the simulated C−N−$C_{str}$ and C═$C_{PDA}$ mode peaks to experiment (Figure 3) imply good fits of the $\nu_{s}$(C═O) peak. Clearly, this is not the case; while the simulated intensity of the Δ[$\nu_{s}$(C═O)] mode peak (∼1774 $cm^{-1}$) is within 8% of the observed value for the 171.0 nm film, the corresponding intensity for the 7.6 nm film is 35% too large. This variability is consistent with the earlier observation that the Δ[$\nu_{s}$(C═O)] peak is sensitive to perturbations in the imide ring structures (Section 3.2.1). In accordance with this behavior, the simulated intensity of the Δ[$\nu_{as}$(C═O)] peak is also too intense, by a factor of ∼2 for both films.

Simulations also were made to check the out-of-plane character of the imide rings in the buffed films as manifested in the normal incidence Δ spectra of the C−N−$C_{bend}$ mode peak in Figure 3 (inset). Since this mode has a *z* direction transition moment, one expects Δ(C−N−$C_{bend}$) to equal 0. The observation of Δ(C−N−$C_{bend}$) < 0 can occur only if the imide rings in a realigned domain are twisted out of the surface plane relative to the initial state. Determination of the average twist angle is desirable, but accurate modeling is precluded because the initial state is poorly defined. This situation follows from our earlier observation that only regions of initially unperturbed, planar imide rings are affected by the buffing process and neither the actual fraction of these regions nor the imide ring twist angles are known with much accuracy. An approximate simulation of the C−N−$C_{bend}$ mode peak was made by constructing the optical tensor from the in-plane C−N−$C_{bend}$ optical function, $\hat{n}(\nu)_{in}$. It was assumed that the imide rings are isotropic in the *z* direction, viz., an average out-of-plane twist of ∼45° (based on our estimates of the ring structures in the 3 $\mu$m free-standing film from which $\hat{n}(\nu)_{in}$ was derived originally[13]). Thus, the magnitude of the out-of-plane matrix elements were set equal to the in-plane values. The C−N−$C_{bend}$ spectra then were simulated using the same realignment layer thicknesses used for the other modes, as described above. The resulting best fits shown in Figure 3 represent imide ring twists of ∼30°.

A similar estimate of buffing-induced, out-of-plane imide ring twist can be made from the $\upsilon_{as}$(C═O) peaks in Figure 3. We observe that these simulated intensities do not fit very well compared to the C−N−$C_{str}$ and C═$C_{PDA}$ fits. Since the $\upsilon_{as}$(C═O) mode has a *y* direction transition moment, the intensity of this peak will decrease in the Δ spectra as a function of increasing imide ring twist as the [O═C−N−CdO] moiety is rotated out of the x,y plane (Figure 1). The thicknesses of the alignment layers were fixed to the values obtained from the C−N−$C_{str}$ and C═$C_{PDA}$ fits, and simulations were made for the 7.6 and 171.0 nm films in which the out-of-plane imide ring twist was varied, a variation that does not affect the C−N−$C_{str}$ and C═$C_{PDA}$ fits. The best fit to the $\upsilon_{as}$(C═O) peak occurs for a twist of ∼40 ± 4°. This value should be considered approximate since the rubbing process induces a high degree of structural perturbation relative to the initial state and the $\upsilon_{as}$(C═O) peak actually consists of several components of varying oscillator strengths. This is in agreement with the multiple peaks observed in the drawn film spectra (Section 3.2.3).

## 4. Discussion

The essential elements that describe the structural effects of buffing of supported BPDA-PDA films under our conditions are summarized graphically in Figure 2. The main features are the realignment of polymer chains and the surface region sensitivity of the process. We first will discuss these two aspects in order and then proceed to an overall picture of the microscopic details of the process.

**4.1. Characteristics of the Buffing-Induced Structural Changes.** *4.1.1. Ring Distortions and Decay of Interchain Ordering.* The most obvious feature of the buffing response is the alignment of polymer chain axes parallel to the rubbing direction, established firmly by GIXRD studies[4] and confirmed conclusively by the IR data. On the basis of the Δ spectra given in Figure 3, we conclude (Section 3.2.1) that unidirectional buffing not only aligns the chains but produces perturbed imide ring structures, in addition to those that are intrinsic to the unbuffed state.[13] From the data in Figures 4−6 and the analysis in Table 2, we conclude further that the perturbed and unperturbed imide rings in the unbuffed samples exist predominantly in separate domains and that only the unperturbed imide domains are responsive to the rubbing process (Section 3.2.2). These data suggest that alignment induces secondary disruption of structure. The published GIXRD results of Toney et al. also can be interpreted to show such effects.[4] In particular, their data establish that, while the realigned chains remain ordered in terms of repeat unit spacing, the periodic chain−chain spacing within the realigned stacking planes decays.[22] Combining the IR and GIXRD data defines a buffing process in which domains of well-ordered, rodlike chains, with uniform spacings and highly planar backbone rings, rotate in-plane to align with the buffing direction. Accompanying this process are distortions of the rings with a broadening of interchain spacings and thus a decay of the interchain order parameter. The distortions of the imide rings include variable extents of out-of-plane twisting around the chain axis; from the simulation-based analysis of the out-of-plane C−N−$C_{bend}$ mode IR spectra (Figure 3 Section 3.3), average values of ∼30−45° are reasonable. One can note that there is no $C_2$ rotation axis in the benzimide moiety. Since the repeat unit spacing remains quite periodic (GIXRD result) after buffing, in order that ring twisting around the C−N (∼chain axis) bond not alter the repeat unit spacing the imide ring must buckle or distort asymmetrically.

*4.1.2. Amount of Material Responsive to Buffing.* Application of the surface selective GIXRD[4] and NEXAFS[5] probes has established that the buffing response in BPDA-PDA films is

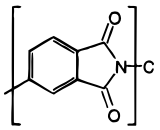

restricted to an ∼5−10 nm near-surface region. The IR probe used in the present paper is not surface selective but is able to quantitate the amount of polymer involved in the realignment. If one assumes that all the polymer involved is contained in contiguous layers at the polymer surface, as illustrated in Figure 2B, simulation-based analysis of the data in Figure 3 gives a response layer thickness of ∼1.8−2.8 nm or an average value of ∼2.3 nm. However, these must be minimum values since the IR data also establish that not all domains respond to buffing, viz., domains containing perturbed imide rings are generally unaffected. Further, it is reasonable to assume that the perturbed and unperturbed ring domains in the unbuffed sample are distributed uniformly throughout the stacking layers at all depths, so a knowledge of the fraction of responsive domains would then allow calculation of a response depth. Since exact quantitation of the fraction of the responsive initial domains is not possible from our data, one cannot calculate the exact response depth. However, average values within the range of ∼1.8−5.6 would be reasonable, in excellent agreement with the GIXRD and NEXAFS upper limits.[23]

*4.1.3. Picture of the Buffed Surface and Possible LC Alignment Mechanisms.* When the elements of the above conclusions are combined, the picture emerges of the buffing process producing a *molecularly roughened surface* consisting of two types of polymer domains: (1) those that consist of intrinsically perturbed ring structures, which did not reorient upon buffing and remain randomly oriented in-plane and (2) those with initially well-ordered chains that realigned on buffing. The reoriented domains exhibit a roughening perpendicular to the chain axes, caused by the decay of the interchain periodicity, and a roughening parallel to the chains caused by a modulation of the localized out-of-plane twisting and buckling of imide groups along the chains. Further, since this localized disordering places some fraction of the C═O groups at angles to the surface plane, the dipolar electrical character of the surface will be perturbed. We point out that these new aspects of the buffing process may be of considerable importance in developing an understanding of the presently poorly defined role of buffing in liquid crystal alignment in display applications,[1] as has recently been speculated by other workers for the case of an amorphous polyimide.[8] We note the parallel of this localized surface roughening with the types of localized variations in molecular topography involving conformationally disordered alkyl chains that has recently been put forward to explain LC alignment effects on self-assembled monolayer surfaces.[10]

**4.2. Buffing Mechanism and the Intrinsic BPDA-PDA Structure.** While the above discussion has summarized important characteristics of the buffing-induced structural changes at BPDA-PDA film surfaces, the issues of the underlying correlations between these changes and the intrinsic polymer structures remain.

*4.2.1. How Does Chain Motion Occur on Buffing?* First we discuss the issues of how polymer motion occurs well below the bulk glass transition temperature, $T_g^{bulk}$, estimated to be at least 400 °C,[4] and why the motion is rotational with no observed loss of material. For the molecular groups in the surface regions of BPDA-PDA to undergo in-plane rotations, independent of the remainder of the film, the stacking planes must be capable of some degree of independent response to in-plane linear shear forces. Further, some mechanism must be available to convert the linear force to a rotational response. A limiting example of a high interplanar shear response is given by graphite, for which the aromatic planes are separated by 3.40 Å and exhibit a registry phase shift.[24] In the case of a perfect, minimum-energy BPDA-PDA structure, the stacking plane spacings are predicted to be near 3.5 Å with an ∼0.2 nm shift in vertical registry.[25,26] At these interplanar distances no covalent bonding can exist between atoms in different layers and the interplanar attractive potentials are controlled by van der Waals interactions. If the BPDA-PDA film structure were as perfect as graphite, then application of unidirectional in-plane shear forces would be expected to cause nearly independent, *linear* sliding motion of all the stacking planes as single units to the point that material is removed from the film surface. The fact that this does not occur under our rubbing conditions is due to two factors. First, the PI stacking planes consist of many domains with different collective chain axis orientations. However, if the stacking planes were held only by van der Waals forces, then one still would expect a linear slip between planes with all domains responding as a unit. Thus, the second factor must be that there are localized interconnections between contiguous domains in adjacent shear planes, most likely via isolated, shared defect PI chains that behave as interplanar cross links. In this case, these domains are strongly pinned to one another at isolated localities and a component response of the applied linear in-plane force would be rotational motion around the pinning centers. On the basis of the observation that the chains always reorient parallel to the buffing direction, it is obvious that the frictional response of the domain surfaces is highly anisotropic with the lowest friction along the chain axes. The fact that the domains appear to reorient independently suggests that the interdomain defect regions within a stacking plane do not exert strong coupling forces between the domains. Since the domain rotations, at least to a first approximation (see below), do not involve independent chain motions within each domain, the motion should not require heating to $T_g^{bulk}$, consistent with experiment. One can consider the possibility of a local surface glass transition temperature, $T_g^{surf}$, lying somewhat above ambient temperature but well below $T_g^{bulk}$.[27] In this case, localized heating above $T_g^{surf}$ during rubbing could cause chain alignment followed by a fast quenching to leave a frozen, aligned surface layer. This phenomena for the BPDA-PDA thin films is discounted by an additional experiment we performed in which a rubbed film was subsequently heated to 350 °C, presumably well above any possible local $T_g^{surf}$ values, and the spectrum was remeasured. It was observed that the thickness of the reorientation layer actually *increased* slightly (near 10%), similar to the relaxation behavior of the drawn, free-standing films in Figure 8. This behavior is analogous to that recently reported for buffed polystyrene.[28] The failure of the film surface structure to randomize demonstrates the lack of any thermally induced segmental disordering. Finally, it follows from the domain pinning model that one would expect a gradual decay of the coupling of the frictional response of the top surface layer to the lower layers, as is observed,[5] with the decay strongly dependent on the density of the stacking plane interconnects. The fact that our observed buffing response thicknesses are fairly independent of the total film thicknesses indicates that in our samples the average density of stacking plane domain interconnects must be similar.

*4.2.2. Why Do Imide Rings Restructure on Buffing?* Next, we discuss the issue of why ring structure perturbations arise on buffing. Since both IR and GIXRD show buffing induces some disruption of the packing of the chains and the planarity

of the backbone rings in initially well-ordered domains, it is clear that some degree of relative motion must occur between adjacent chains within each reorienting domain. This would seem to arise by the applied shear forces causing the chain axes to slide slightly out of registry with one another during in-plane rotation of the domain. With reference to Figures 1 and 2, in a well-ordered domain of extended zigzag chains, the ring groups along adjacent chains are staggered along the *x* direction. Even small relative displacements of the chains along *x* would cause unfavorable steric interactions between neighboring rings, with the result of ring distortions and small variations in the chain−chain spacings. The highest stress points of these interactions will arise between adjacent [O═C−N−C═O] moieties since these extend furthest away from the chain axes (see Figure 1) and thus the largest structural perturbations would be expected here. These essential features of this response are represented in the cartoons in Figure 2A.

*4.2.3. Why Are Initially Perturbed Domains Unresponsive to Buffing?* Finally, we discuss the issue of the why domains of initially disrupted structures appear relatively unresponsive to buffing. This effect is clearly seen for the thicker films in Figure 3, for the 9.0 nm film in Figure 7, and generally by the absence of the $\nu^*_{as}$(C═O) mode in the Δ|| spectra in Figure 4. The IR data establishes that unbuffed, ultrathin BPDA-PDA films, made in the identical way as those shown previously to be well-ordered by X-ray diffraction,[4] exhibit a significant fraction of imide rings with perturbed structures. These perturbations must arise from the inability of the polyimide chains to anneal completely at the imidization temperature. This effect is a result of the rise of $T_g^{bulk}$ above the curing temperature as imidization progresses to leave kinetically trapped defects such as cross-links and trace anhydride formation that interrupt the chain packing[29] and distort [O═C−N−C═O] units. It follows that the regions containing these defects will have an entangled, three-dimensional nature with a significant degree of covalent stacking plane interconnects. Such structures will be highly resistant to permanent deformation when the applied shearing forces are below what is required to rupture the interconnected chain segments. In view of the large in-plane tensile strengths of BPDA-PDA, these thresholds will be quite large.

## 5. Conclusions

A molecular mechanism for polyimide chain alignment during unidirectional rubbing in polyimide thin films at ambient temperatures has been formulated based on quantitative infrared spectroscopy. The observation of reversible chain segmental motion several hundred degrees below the bulk glass transition temperature is explained in terms of a conversion of the linear shear force into a collective chain rotational motion of well-ordered domains around pinning centers that interconnect adjacent stacking planes via defect polyimide chains. Domains that are initially of low order are resistant to realignment, presumably because of extensive three-dimensional defects that preclude shear response. The domain rotation is further proposed to induce a slight relative linear sliding of adjacent chains that causes deformations of the imide ring structures and decay of the chain−chain translational ordering as unfavorable interchain steric interactions arise. The deformations include contributions from both changes in the imide group bonding and out-of-plane twisting of the rings, with the contributions dependent on the initial degree of ordering of the domain and the overall response being equivalent to a "molecular roughening" of the film surface. The response is proposed to decay with depth into the film, and the infrared data show, consistent with published GIXRD and NEXAFS studies, involvement of a nearly constant amount of film material equivalent to an ∼ 1−3 nm surface layer. An analogue of the domain reorientation is given by unaxially drawn, free-standing films at ambient temperature where similar chain reorientation and imide ring deformations are observed. The formulation of this new mechanism for buffing response provides a more complete picture than previously available for developing detailed mechanisms of liquid crystal alignment on buffed polyimide film surfaces.

**Acknowledgment.** Discussions with S. K. Kumar are gratefully acknowledged. Financial support was obtained from the National Science Foundation (GOALI program, DMR-9631512) and the Army Research Office (AASERT program, DAAL03-92-G-0090).

## References and Notes

(1) Patel, J. S. *Annu. Rev. Mater. Sci.* **1993**, *23*, 269−294.

(2) Bahadur B. *Liquid Crystals; Applications and Uses*; World Scientific, 1992; Vol. 3.

(3) (a) van Aerle, N. A. J. M.; Tol, A. J. W. *Macromolecules* **1994**, *27*, 6520−6526. (b) Sakamoto, K.; Arafune, R.; Ito, N.; Ushioda, S.; Suzuki, Y.; Morokawa, S. *J. Appl. Phys.* **1996**, *80*, 431−439. (c) Sawa, K.; Sumiyoshi, K.; Hirai, Y.; Tateishi, K.; Kamejima, T. *Jpn. J. Appl. Phys.* **1994**, *33*, 6274−6276. (d) van Aerle, N. A. J. M.; Barmentlo, M.; Hollering, R. W. J. *J. Appl. Phys.* **1993**, *74*, 3111−3120. (e) Seo, D. S.; Oh-Ide, T.; Matsuda, H.; Isogami, T. R.; Muroi, K. I.; Yabe, Y.; Kobayashi, S. *Mol. Cryst. Liq. Cryst.* **1993**, *231*, 95−106. (f) Ishihara, S.; Wakemoto, H.; Nakazima, K.; Matsuo, Y. *Liq. Cryst.* **1989**, *4* (6), 669−675. (g) Geary, J. M.; Goodby, J. W.; Kmetz, A. R.; Patel, J. S. *J. Appl. Phys.* **1987**, *62*, 4100−4108.

(4) Tony, M. F.; Russell, T. P.; Logan, J. A.; Kikuchiu, H.; Sands, J. M.; Kumar, S.K. *Nature* **1995**, *374*, 709−711.

(5) Samant, M. G.; Stohr, J.; Brown, H. R.; Russell, T. P.; Sands, J. M.; Kumar, S. K. *Macromolecules* **1996**, *29*, 8334−8342.

(6) Sun, R.; Guo, J.; Huang, X.; Ma, K. *Appl. Phys. Lett*. **1995**, *66*, 1753−1754. Sakamoto, K.; Arafune, R.; Ushioda, S.; Suzuki, Y.; Morokawa, S. *Jpn. J. Appl. Phys*. **1994**, *33*, L1323−1326.

(7) Hietpas, G. D.; Sands, J. M.; Allara, D. L. *Macromolecules* **1998**, *31*, 3374−3378.

(8) Stöhr, J.; Samant, M. G.; Cossy-Favre, A.; Diaz, J.; Momoi, Y.; Odahara, S. *Macromolecules* **1998**, *31*, 1942−1946.

(9) Weiss, K.; Wöll, C.; Böhm, E.; Fiebranz, B.; Forstmann, G.; Peng, B.; Scheumann, V.; Johannsmann, D. *Macromolecules* **1998**, *31*, 1930−1936.

(10) Drawhorn, R. A.; Abbott, N. L. *J. Phys. Chem*. **1995**, *99*, 16511−16515. Gupta, V. K.; Abbott, N. L. *Langmuir* **1996**, *12*, 2587−2593. Gupta, V. K.; Miller, W. J.; Pike, C. L.; Abbott, N. L. *Chem. Mater*. **1996**, *8*, 1366−1369.

(11) Sroog, C. E. *Prog. Polym. Sci.* **1991,** *16*, 561−694. Verbicky, J. W. *Encyclopedia of Polymer Science and Engineering*, 2nd ed.; Wiley and Sons: New York, 1988; Vol.12, p 364.

(12) Ishida, H.; Huang, M. T. *Spectrochim. Acta* **1995**, *51A*, 319. Ishida, H.; Wellinghoff, S. T.; Baer, E.; Koenig, J. L. *Macromolecules* **1980**, *13*, 826−834.

(13) Hietpas, G. D.; Allara, D. L. *J. Polym. Sci., Polym. Phys. Ed*. **1998**, *36*, 1247−1260.

(14) This correction has not been specifically mentioned in previous polarized infrared studies on rubbed polyimide films (see refs 3a−d). However, as a result of the more flexible nature of the polyimides in these studies, larger orientation layers were formed and contributions from $[I(||)_U - I(\perp)_U]$ would have likely been too small to affect the shape of the reported, uncorrected $[I(||)_B - I(\perp)_B]$ difference spectra.

(15) Yeh, P. *Optical Waves in Layered Media;* Wiley-Interscience: New York, 1988.

(16) Parikh, A. N.; Allara, D. L. *J. Chem. Phys.* **1992**, *96*, 927−945.

(17) Ree, M.; Chu, C. W.; Goldberg, M. J. *J. Appl. Phys.* **1994,** *75*, 1410−1419. Yoon, D. Y.; Parrish, W.; Depero, I. E.; Ree, M. *Mater. Res. Soc. Symp.* **1991**, *227*, 387−393. Herminghaus, S.; Boese, D.; Smith, B. A. *Appl. Phys. Lett.* **1991,** *59*, 1043−1045.

(18) The optical constants necessary to this calculation for $SiO_2$ and Si were taken from the following: Palik, E. D. *Handbook of Optical Constants of Solids;* Academic Press: New York, 1985. The tabulated values obtained were interpolated by a cubic spline fit in the frequency region of interest.

(19) The deviation in this behavior for the 4.7 nm film is due to the fact that, for films 2−5 nm, the films are highly dependent on preparation

conditions and usually contain a larger fraction of perturbed imide rings than films slightly thicker, near 7−10 nm. This behavior can also be shown in Figure 6.

(20) Smirnova, V. Y.; Bessonov, M. I.; Sklizkova, V. P. *Polym. Sci. U. S. S. R.* **1990**, *32*, 267−271.

(21) Jackson, M.; Mantsch, H. H. *Crit. Rev. Biochem. Mol. Biol.* **1995**, *30*, 95−120.

(22) Specifically, the observation of a sharp (004) peak when the scattering vector (**Q**) is parallel to the rubbing direction shows the chains remain in an extended zigzag conformation with a 3.1 nm repeat unit spacing along the chain axis. However, when **Q** is perpendicular to the chain axis, the associated peak shows a large increased intensity and broadening, indicating a decay of the interchain ordering away from the periodic value of ∼0.6 nm.

(23) An important point that appears to have been missed in previous X-ray characterization studies is that the actual magnitude of the buffing response increases directly with an increase in the initial state of ordering of the BPDA-PDA film (Section 3.3). Thus, buffing-induced structural changes must be correlated with the initial state of the selected sample in order to obtain statistically meaningful results.

(24) Pauling, L. *The Nature of The Chemical Bond*, 3rd ed.; Cornell University Press: Ithaca, NY, 1960.

(25) Poon, T. W.; Silverman, B. D.; Saraf, R. F.; Rossi, A. R. *Phys. Rev. B* **1992,** *46* (18), 11456−11462.

(26) Silverman, B. D. *Macromolecules* **1989,** 22, 3768.

(27) The existence of a unique surface glass transition temperature has become a contentious issue recently. A brief summary is given by Russell and co-workers (Liu, Y.; Russell, T. P.; Samant, M. G.; Stöhr, J.; Brown, H. R.; Cossy-Favre, A.; Diaz, J. *Macromolecules* **1997**, *30*, 7768−7771). These authors show that room-temperature buffing of polystyrene produces a surface layer of oriented chains but that upon heating the onset of orientational relaxation only occurs at $\sim T_g^{bulk}$. This evidence discounts the existence of a unique $T_g^{surf}$ but shows that chain realignment in an amorphous polymer can occur below $T_g^{bulk}$.

(28) In the study in ref 27, a room-temperature-buffed polystyrene sample heated to 40 °C actually showed an increase in chain orientation. Russell and co-workers ascribe this to a relaxation of stresses and bond angle distortions arising within the film during rubbing.

(29) Pryde, C. A. *J. Polym. Sci., Part A: Polym. Chem.* **1989**, *27*, 711−724.